environmental microbiology

Environmental Microbiology (2014) **16**(4), 1137–1149 doi:10.1111/1462-2920.12358

Novel molecular determinants of viral susceptibility and resistance in the lipidome of *Emiliania huxleyi*

James M. Fulton,[1*†] Helen F. Fredricks,[1] Kay D. Bidle,[2] Assaf Vardi,[3] B. Jacob Kendrick,[4] Giacomo R. DiTullio[4] and Benjamin A. S. Van Mooy[1]

[1]*Department of Marine Chemistry and Geochemistry, Woods Hole Oceanographic Institution, Woods Hole, MA, USA.*

[2]*Environmental Biophysics and Molecular Ecology Laboratory, Institute of Marine and Coastal Sciences, Rutgers University, New Brunswick, NJ, USA.*

[3]*Department of Plant Sciences, Weizmann Institute of Science, Rehovot, Israel.*

[4]*Hollins Marine Laboratory, College of Charleston, Charleston, SC, USA.*

Summary

Viruses play a key role in controlling the population dynamics of algae, including *Emiliania huxleyi*, a globally distributed haptophyte with calcite coccoliths that comprise ca. 50% of the sinking carbonate flux from the surface ocean. *Emiliania huxleyi* viruses (EhVs) routinely infect and terminate *E. huxleyi* blooms. EhVs are surrounded by a lipid envelope, which we found to be comprised largely of glycosphingolipids (GSLs) with lesser amounts of polar glycerolipids. Infection appears to involve membrane fusion between the virus and host, and we hypothesized that specific polar lipids may facilitate virus attachment. We identified three novel intact polar lipids in *E. huxleyi* strain CCMP 374 and EhV86, including a GSL with a monosaccharide sialic acid headgroup (sGSL); for all 11 *E. huxleyi* strains we tested, there was a direct relationship between sGSL content and sensitivity to infection by EhV1, EhV86 and EhV163. In mesocosms, the *E. huxleyi* population with greatest initial sGSL content had the highest rate of virus-induced mortality. We propose potential physiological roles for sGSL that would be beneficial for growth but leave cells susceptible to infection, thus furthering the discussion of Red Queen-based co-evolution and the cost(s) of sensitivity and resistance in the dynamic *E. huxleyi*-EhV system.

Introduction

Viruses are abundant (10^7 to 10^{11} virions l^{-1} seawater) and active components of the marine ecosystem (Wilhelm and Suttle, 1999). Virus infection contributes to biogeochemical nutrient cycles and marine food webs by inducing cell lysis and shunting nutrients and organic carbon to microbial food webs and away from zooplankton and higher trophic levels (Fuhrman, 1999; Suttle, 2007; Brussaard *et al*., 2008). The resultant increase in microbial respiration has the effect of diminishing the 'biological pump' that exports organic carbon to the deep ocean (Fuhrman, 1999). The overall impact of virus infection on biogeochemical cycles is more complex, however, and additional feedback mechanisms must be considered (Brussaard *et al*., 2008), such as the recent observation of enhanced production of transparent exopolymer particles (TEPs) in infected populations of *Emiliania huxleyi* (Prymnesiophyceae, Haptophyta) (Vardi *et al*., 2012). Increased TEP production provides a mechanism for viruses and infected cells to become bound in marine snow, which could reduce infectivity, stimulate vertical sinking flux and potentially increase organic carbon export (Passow *et al*., 2001; Vardi *et al*., 2012). Thus, the global effects of aquatic viral infection and their magnitudes are still being refined, and the development of biomarkers related to viral infection will help delineate the relationships among host populations, viral infection and biogeochemical cycles.

Aquatic viruses of the Phycodnaviridae family (100–220 nm diameter, icosahedral, double-stranded DNA viruses) infect diverse algae and include the *E. huxleyi* viruses (EhVs), also called coccolithoviruses (Schroeder *et al*., 2002; Wilson *et al*., 2009). EhVs have been shown to play a significant role in terminating massive *E. huxleyi* blooms in the English Channel, a Norwegian fjord, and the North Sea (Bratbak *et al*., 1993; Wilson *et al*., 2002a,b). Furthermore, EhV infection has been implicated to explain a minimum in *E. huxleyi* abundance at an open-ocean site in the North Atlantic (Vardi *et al*., 2009), and induced blooms in enclosed mesocosms containing natural host and virus populations provided further confirmation of the

Received 19 June, 2013; accepted 5 December, 2013. *For correspondence. E-mail james_fulton@baylor.edu; Tel. (+1) 254 710 2158; Fax (+1) 254 710 2673. †Present address: Department of Geology, Baylor University, Waco, TX, USA.

role that EhVs can play in terminating *E. huxleyi* blooms (Bratbak *et al*., 1993; Bidle *et al*., 2007; Bidle and Kwityn, 2012; Vardi *et al*., 2012).

Recent culture- and field-based experiments have indicated that membrane lipids play a central role in *E. huxleyi*-EhV interactions (Vardi *et al*., 2009; 2012; Bidle and Vardi, 2011). The genome of EhV86, the type coccolithovirus, contains a nearly complete sphingolipid synthesis pathway (Wilson *et al*., 2002b; 2005), and isolated EhV86 virions were found by mass spectrometry to contain glycosphingolipids (GSLs) (Vardi *et al*., 2009). In a separate microscopy-based study, Mackinder and colleagues (2009) suggested that EhV86 is surrounded by a lipid envelope, a novel feature among the Phycodnaviridae, and proposed that the virus enters *E. huxleyi* cells by endocytosis or membrane fusion with the host plasma membrane. These entry mechanisms are typical of animal viruses that utilize specific membrane components such as glycan-binding lectins and glycan-hydrolysing sialidases to promote viral attachment, entry and release (Stray *et al*., 2000; Varki, 2008; Varki and Schauer, 2009). The EhV86 genome provides enticing evidence supportive of an animal-like, lipid-membrane-dependent infection strategy, as it encodes two C-type lectin domain-containing proteins (ehv060 and ehv149) and a sialidase (ehv455) that might have critical roles in attachment and entry (Wilson *et al*., 2005; Allen *et al*., 2008; Mackinder *et al*., 2009).

EhV86 appears to acquire its lipid envelope by budding through intact host membranes (Mackinder *et al*., 2009), even though massive viral release by host cell lysis is also a prominent characteristic of late-phase *E. huxleyi* infections (Bidle and Vardi, 2011). Following other viral lipidomic studies (Scheiffele *et al*., 1999; Brugger *et al*., 2006), the EhV86 lipidome, which includes GSLs (Vardi *et al*., 2009), may reflect the composition of the host plasma membrane at the point of exit. Uninfected *E. huxleyi* contains polar glycerolipids (glycolipids, phospholipids and betaine lipids; Bell and Pond, 1996), which are the primary structural components of intracellular and plasma membrane lipid bilayers. GSLs, although not previously quantified in *E. huxleyi*, nonetheless appear to have important roles in cell signalling connected to viral infection (Vardi *et al*., 2009; 2012; Bidle and Vardi, 2011), and infection-induced GSL production and localization in lipid rafts appears to facilitate EhV budding (Rose *et al*., 2014). EhVs may acquire additional lipids from intracellular locations, such as C37 and C38 alkenones from lipid bodies (Eltgroth *et al*., 2005), which could function as viral assembly sites, similar to endoplasmic reticulum (ER)-associated lipid droplets in hepatitis C viral replication (Herker and Ott, 2011).

Here, we present the first detailed lipidome analysis of both a coccolithovirus (EhV86) and infected *E. huxleyi* host population (CCMP 374; *Ehux374*). We also analysed the lipid content of additional, uninfected model strains (*Ehux373*, *Ehux379*, *Ehux1516* and *Ehux2090*), as well as 22 *E. huxleyi* strains recently isolated from an induced-bloom mesocosm experiment in a Norwegian fjord (Hinz, 2010). For 11 strains that were also screened for infection sensitivity, we found a direct relationship between susceptibility to infection and the occurrence of novel GSLs with a sialic acid headgroup. Both intact polar lipids (IPLs) and alkenones detected in purified EhV86 were also found in the host, although with significant differences in relative abundance, suggesting that the EhV membrane is derived from lipids of particular host cell compartments. We outline potential roles for the sialic acid-containing GSL in viral infection and *E. huxleyi* physiology, and based on its distribution in a diverse range of host strains and natural populations of isolated mesocosms, we propose its use as an environmental biomarker to assess *E. huxleyi* population sensitivity to EhV infection.

Results and discussion

Lipids in Ehux374 during infection

In laboratory cultures, growth of *Ehux374* during infection by the lytic virus EhV86 was similar to that reported previously (Bidle *et al*., 2007; Vardi *et al*., 2009). Average counts from triplicate bottles increased from $3.28 \pm 0.03 \times 10^5$ to $4.53 \pm 0.07 \times 10^5$ cells ml^{-1} during the first day after inoculation with the viral lysate, then gradually decreased to $1.45 \pm 0.16 \times 10^5$ cells ml^{-1} at the end of the experiment, 4 days post-infection (DPI) (Fig. 1A). In contrast, the uninfected control cultures remained in exponential growth and increased to a maximum of $1.12 \pm 0.02 \times 10^6$ cells ml^{-1}, nearly 10-fold higher than the final infected population. The steady decrease in the infected *Ehux374* population from 1 to 4 DPI resulted from virus-induced cell lysis, and the residual population, similar in concentration to previous studies (Bidle *et al*., 2007; Evans *et al*., 2009; Vardi *et al*., 2009), likely included both infected cells and cells that had developed stable coexistence with EhV86 (Thyrhaug *et al*., 2003), the nature of which is currently unknown. Thus, it is possible that some of the observed changes in lipid distributions near the end of the experiment (4 DPI) might have been influenced by an infection-resistant subpopulation. The plateau in EhV abundance at 2 DPI has been observed previously (Bidle *et al*., 2007) and records a decrease in the release rate of new EhVs. Nonetheless, as described extensively below, the continued exponential increase in viral GSLs (vGSLs) in the residual *E. huxleyi* population demonstrates that the infection continued to expand (Fig 1B).

Analysis of IPLs by high-performance liquid chromatography-multistage ion trap mass spectrometry

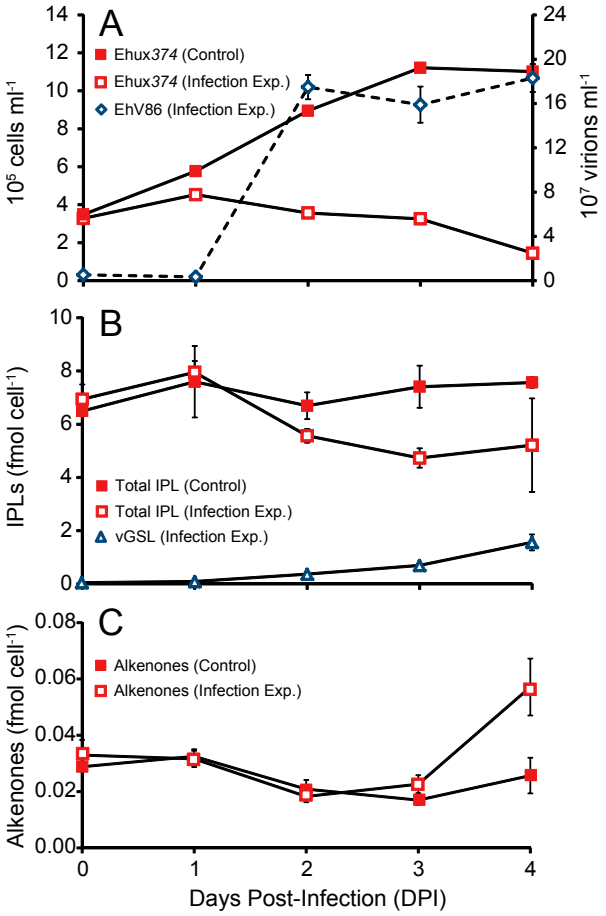

Fig. 1. (A) Time course of cell and virus abundance for uninfected control and infection experiments. (B) Total intact polar lipids and viral glycosphingolipids (vGSLs) in infected and control populations of *Ehux374* in culture. (C) Total C37 and C38 alkenone content in control and infected cultures.

(HPLC-MS^n) (Sturt *et al.*, 2004; Van Mooy and Fredricks, 2010) showed an overall reduction in lipid content in infected cultures. IPLs, which are primarily associated with membranes, decreased from 8.0 ± 0.4 fmol cell^{-1} to 5.2 ± 1.8 fmol cell^{-1} between 1 and 4 DPI (Fig. 1B). This change in total IPL content was driven primarily by a loss of glycolipids of the thylakoid membrane that was only partially offset by an increase in GSLs associated with the plasma membrane (Fig. 2). C37 and C38 alkenones, which are thought to reside primarily in lipid bodies (Eltgroth *et al.*, 2005), were analysed by gas chromatography and found to represent a small component of the overall lipidome that only varied appreciably after 4 DPI (Fig. 1C). Sterols and triacylglycerides are generally present in only trace amounts (Yamamoto *et al.*, 2000) and were not analysed for this study. Overall, the lipid data we collected show that viral infection resulted in large shifts in the quantity and types of lipids in *E. huxleyi* and that the preponderance of these changes occurred in membranes.

GSLs. We identified three classes of GSLs in *Ehux374* during EhV infection, two of which were classified previously as viral (vGSLs) and host GSLs (hGSLs) because of their prevalence in infected and uninfected *E. huxleyi* respectively (Vardi *et al.*, 2009; 2012). Both hGSL and vGSL have a glycosyl headgroup, but hGSL has a methylated d19:3 long-chain base (LCB) (Vardi *et al.*, 2012) and vGSL has a distinctive 16:1 tetrahydroxy LCB (Vardi *et al.*, 2009). We detected hGSLs with unsaturated C22:1, C22:2 and C22:3 hydroxy fatty acids, and during *Ehux374* infection experiments, total hGSL content remained between 0.06 ± 0.01 and 0.11 ± 0.01 fmol cell^{-1} (Fig. 2A). We only detected GSLs with 16:1 tetrahydroxy LCBs in infected cultures, supporting the hypothesis that vGSL production results from the expression of viral genes for sphingolipid biosynthesis (Pagarete *et al.*, 2009; Vardi *et al.*, 2009). The exponential increase in vGSL along with decreasing cell counts indicates that viral gene expression and lytic infection continued to expand through 4 DPI (Fig. 1). Observed vGSLs included species with saturated and mono-unsaturated fatty acid moities ranging from C18 to C24, predominately C22:0 and C22:1; total vGSL concentration increased exponentially to 1.58 ± 0.32 fmol cell^{-1} in infected cultures (Fig. 2A, Supporting Information Table S1).

The third GSL class identified in *Ehux374* was a novel sialic acid GSL (sGSL), a monosialylceramide that appeared to have the sialic acid 2-Keto-3-deoxynonic acid (KDN) as its headgroup (Fig. 3; Supporting Information Appendix S1). We detected two species with different LCBs (d18:1 or d18:2), and both had C22:0 fatty acids, exclusively. Like hGSL, sGSL comprised approximately 50% of the GSLs prior to infection (Fig. 2A). Its concentration was constant at 0.07 ± 0.01 fmol cell^{-1} in uninfected cultures but increased exponentially to 0.42 ± 0.29 fmol cell^{-1} at the end of the infection experiment (Supporting Information Table S1). Increased sGSL did not appear to be the result of a broad, indiscriminate stimulus of all GSLs, as hGSL concentration remained relatively stable in infected cultures. The rate of sGSL increase was less than that of vGSL, whose production depends on a serine palmitoyl transferase that is encoded in the EhV86 genome and shows preference for myristoyl-coenzyme A (Han *et al.*, 2006; Vardi *et al.*, 2009).

Glycolipids. The uninfected *Ehux374* lipidome consisted largely of glycolipids (Fig. 2B) along with other abundant polar glycerolipids including phospholipid and betaine lipid classes that were previously identified in *E. huxleyi* and the marine environment (Bell and Pond, 1996; Kato *et al.*, 1996; Van Mooy *et al.*, 2009; Van Mooy and

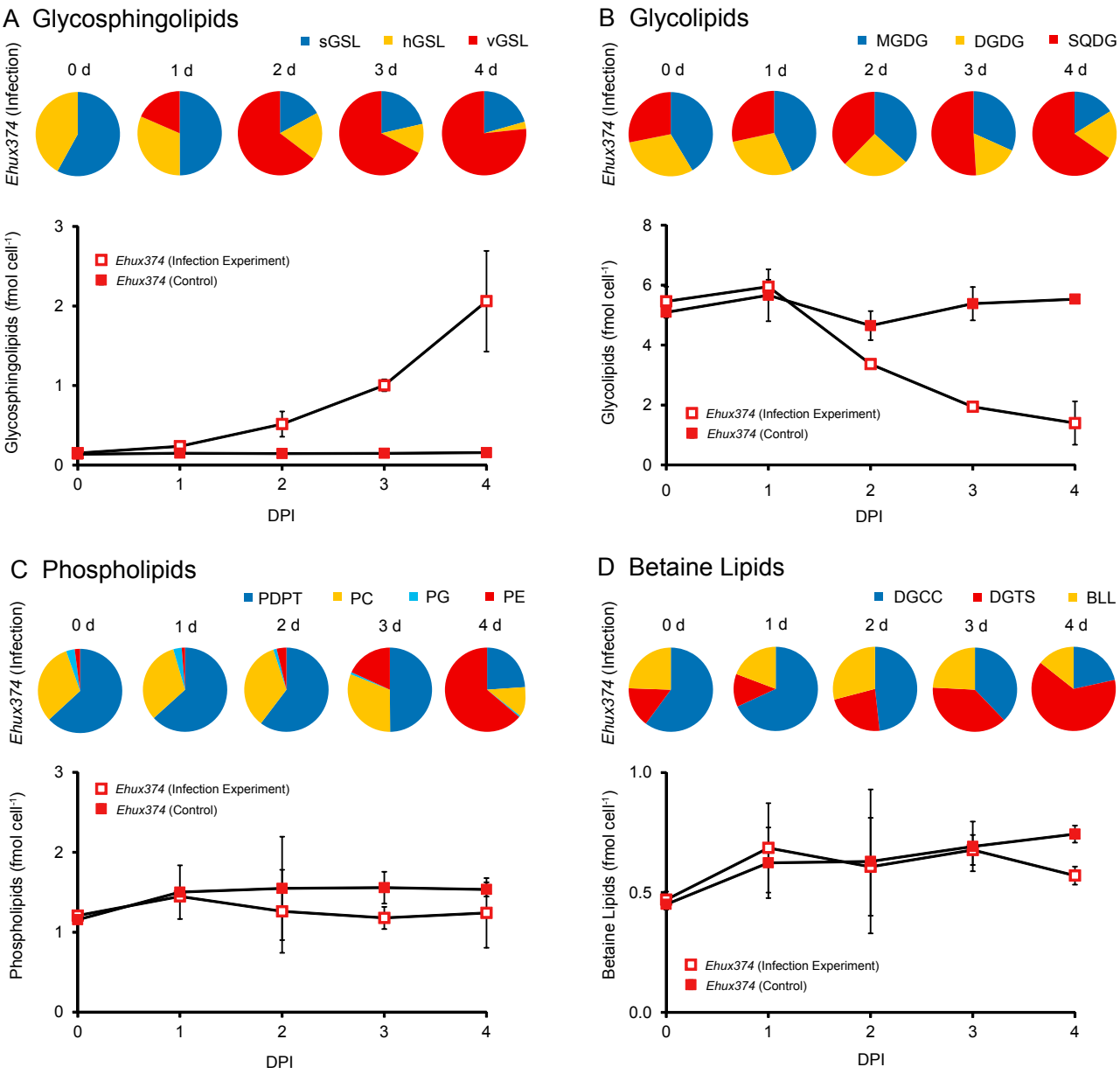

Fig. 2. Shifts in IPL lipidome components during EhV86 infection of *Ehux374*. Pie graphs show the distributions of lipid classes for infected cultures for 0–4 DPI. Lipid distributions did not change significantly in control cultures and resembled the 0 DPI distributions for infected cultures. Glycosphingolipids include sGSL, hGSL and vGSL; glycolipids include MGDG, DGDG and SQDG; phospholipids include PDPT, PC, PG and PE; betaine lipids include DGCC, DGTS and BLL.

Fredricks, 2010). At 4.37 ± 0.09 fmol cell^{-1}, glycolipids made up 65% of the lipidome in uninfected cells, but during infection, glycolipid content decreased to 1.34 ± 0.70 fmol cell^{-1} (Fig. 2B). Monogalactosyldiacylglycerol (MGDG) and digalactosyldiacylglycerol (DGDG) decreased during infection by an order of magnitude from a total of 3.58 ± 0.43 to 0.43 ± 0.24 fmol cell^{-1}. Algal glycolipids are most abundant in the thylakoid membrane, suggesting that the losses of MGDG and DGDG were

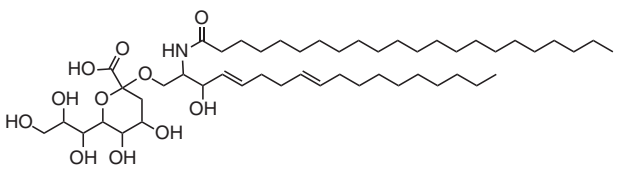

Fig. 3. Tentative sGSL chemical structure. Details of the structural assignments are shown in Supporting Information Figs S1–3. The positions of the double bonds on the LCB are not known.

related to the diminished photochemical capacity associated with infection (Evans *et al*., 2006; Guschina and Harwood, 2006). Evans and colleagues (2009) showed that EhV infection of *E. huxleyi* resulted in decreased content of 18:4 and 18:5 fatty acids, which we found occurred primarily in MGDG and DGDG (Supporting Information Table S2). Sulfoquinivoslydiacylglycerol (SQDG) concentration also decreased, from 1.52 ± 0.05 to 0.91 ± 0.48 fmol cell^{-1}, but its relative content increased during the infection experiment from 30% to 68% of the total glycolipids (Fig. 2B). SQDG shifted from primarily 18:3 and 18:4 fatty acids to 14:0 and 16:0 fatty acids during infection (Supporting Information Table S2), further reducing the content of unsaturated fatty acids as observed by Evans and colleagues (2009).

Phospholipids. Phospholipids comprised 22% of the *Ehux374* lipidome and remained nearly constant during infection with a daily average of 1.27 ± 0.11 fmol cell^{-1} (Fig. 2C). We identified a new sulphur-containing phospholipid class, which was tentatively identified as phosphatidyl-S,S-dimethylpropanethiol (PDPT), similar to phosphatidylsulfocholine found in some diatoms and red algae (Harwood and Jones, 1989), but with the terminal dimethyl sulphide moiety bound to phosphate via propanol instead of ethanol (Supporting Information Appendix S1). We observed large shifts in phospholipid classes during infection, with reductions in PDPT from 0.76 ± 0.02 to 0.30 ± 0.14 fmol cell^{-1}, phopsphatidylcholine (PC) from 0.38 ± 0.02 to 0.14 ± 0.06 fmol cell^{-1} and phosphatidylglycerol (PG) from 0.04 ± 0.01 to 0.01 ± 0.01 fmol cell^{-1}, and a concurrent exponential increase in phosphatidylethanolamine (PE) from trace concentrations to 0.79 ± 0.23 fmol cell^{-1} (Fig. 2C, Supporting Information Table S1).

The increase in PE is perplexing, given that it was only a trace component of uninfected cultures and its production does not appear to be encoded in the EhV86 genome (Wilson *et al*., 2005). In the marine environment, PE is thought to occur primarily in heterotrophic bacteria (Van Mooy and Fredricks, 2010), suggesting possible growth of contaminant bacteria in infected culture medium. However, the distribution of phospholipids does not support this interpretation; marine heterotrophic bacteria in P-replete cultures contain PG along with PE (Van Mooy *et al*., 2009; Popendorf *et al*., 2011), and PG decreased to 0.01 ± 0.01 fmol cell^{-1} during the infection experiment (Fig 2C). Demethylation of the PC headgroup could also produce PE, although PC always had at least one C22:6 fatty acid and PE included only saturated and monounsaturated C14–C18 fatty acids (Supporting Information Table S2), so new PE synthesis was more likely. Evans and colleagues (2009) observed a similar magnitude increase in the same saturated and monounsaturated fatty acids during infection likely explained by an increase in PE in their experiment as well.

Betaine lipids. The betaine lipids diacylglyceryl carboxyhydroxymethylcholine (DGCC) and diacylglyceryl trimethylhomoserine (DGTS) together made up 9% of the uninfected *Ehux374* lipidome and increased from 0.36 ± 0.03 to 0.49 ± 0.05 fmol cell^{-1} during infection, which also resulted in a shift from primarily DGCC to DGTS at the end of the experiment (Fig. 2D). DGTS was not identified previously in *E. huxleyi* (Bell and Pond, 1996; Kato *et al*., 1996); we detected it at 0.08 ± 0.01 fmol cell^{-1} in uninfected *Ehux374*. Like PE, DGTS increased exponentially during infection and included relatively short and saturated fatty acids, predominately the (14:0/18:1) species (Supporting Information Tables S1 and S2). Both PE and DGTS have been identified in a range of algae, and in some green algae, they appear to be co-localized in extraplastidial membranes (Dembitsky, 1996), suggesting that the increased concentration of both of these IPLs could also be linked in infected *E. huxleyi* populations.

We detected a third new lipid, which we classified as a betaine-like lipid (BLL), because it lacked phosphate and contained reduced nitrogen in its headgroup (Supporting Information Appendix S1). BLL and DGCC, along with the phospholipids PDPT and PC, were likely plasma membrane components and included species with the same fatty acid combinations: (14:0/22:6), (16:0/22:6), (18:1/22:6), (22:6/22:6) and trace concentrations of (15:0/22:6) (Supporting Information Table S2). Total BLL had an initial concentration of 0.11 ± 0.01 fmol cell^{-1} that increased to a maximum of 0.18 ± 0.09 fmol cell^{-1} 2 DPI before decreasing to 0.08 ± 0.04 fmol cell^{-1} 4 DPI. Unlike DGCC, PDPT and PC, which each had nearly constant fatty acid distributions during the infection experiment, BLL shifted from being almost exclusively a combination of (16:0/22:6) and (18:1/22:6) species at the start of the experiment to being 50% (22:6/22:6) at the end, 4 DPI (Supporting Information Table S2).

Lipids in the coccolithovirus EhV86

GSLs. GSLs comprised 86% of the EhV86 lipidome (Fig. 4). Consistent with previous work showing significant enrichment of vGSL over hGSL in a virus isolate (Vardi *et al*., 2009), vGSL made up 64% of the IPL lipidome, and sGSL and hGSL accounted for 15% and 7% of the lipidome respectively. Other membrane-bound viruses also contain sphingolipids; in particular, sphingomyelin has been reported as a significant component in the hepatitis C virus, human immunodeficiency virus and influenza viruses (Scheiffele *et al*., 1999; Brugger *et al*., 2006; Merz *et al*., 2011), although it is absent in the *E. huxleyi*-EhV86

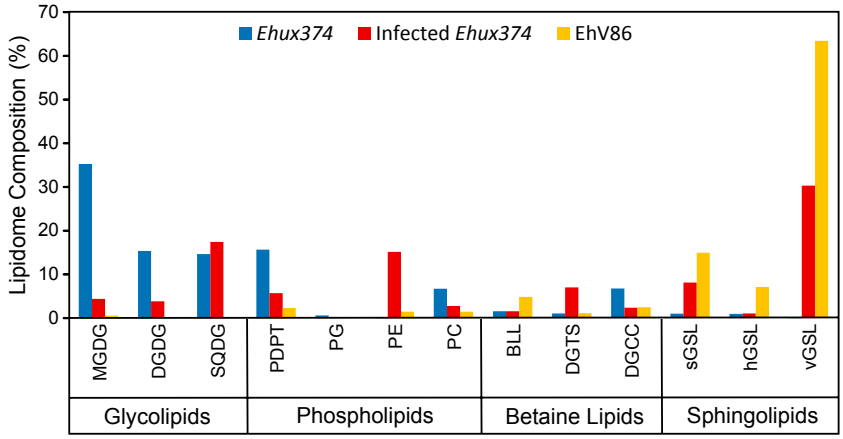

Fig. 4. IPL lipidomes of uninfected *Ehux374*, 4-DPI *Ehux374* and purified EhV86. The *Ehux374* composition is from cells harvested during exponential growth (day 2).

system. EhV86 was enriched in all three GSLs relative to the infected *Ehux374* population at 4 DPI, with vGSL and sGSL showing twofold and hGSL sixfold relative enrichment in the virus (Fig. 4).

Glycolipids, phospholipids and betaine lipids. BLL (4.9%), DGCC (2.5%), PDPT (2.3%), PC (1.5%), PE (1.5%) and DGTS (1.1%) were the most abundant polar glycerolipids in EhV86, but all were minor components compared with the GSLs (Fig. 4). MGDG and SQDG were detected at trace concentrations in EhV86, and DGDG and PG were not detected. BLL was the only polar glycerolipid with a greater relative concentration in EhV86 compared with 4-DPI *Ehux374*, and the (22:6/22:6) fatty acid species in particular comprised 83% of BLL in the virus isolate (Fig 4; Supporting Information Table S2). Over the course of infection the BLL (22:6/22:6) species increased exponentially to 0.04 fmol cell^{-1} (Supporting Information Table S1), when it was 50% of the total BLL content but still a minor component of 4-DPI *E. huxleyi*. Given that it was essentially absent in uninfected *Ehux374*, increased exponentially during the infection experiment, and was fivefold more abundant in EhV86 relative to 4-DPI *Ehux374*, the increased concentration of the BLL (22:6/22:6) species appeared to result directly from infection.

The EhV86 genome encodes a putative transmembrane fatty acid elongation protein (ehv077) that is expressed during infection (Wilson *et al.*, 2005), possibly explaining the increase in BLL (22:6/22:6) in the infected *Ehux374* population. Unlike BLL, the plasma membrane components PC, PDPT and DGCC had mostly (14:0/22:6) and (22:6/22:6) fatty acids regardless of infection status (Supporting Information Table S2). Further, the fatty acid distributions of PC, PDPT and DGCC in EhV86 were the same as in 4-DPI *Ehux374*, suggesting that these lipids had the same fatty acid compositions at the site of EhV assembly and throughout the cell. Thus, it appears that BLL (22:6/22:6) was concentrated specifically at a virus assembly site, and EhV86 acquired it preferentially compared with the other BLL species and polar glycerolipids of the plasma membrane.

GSLs in virus assembly. The similar twofold enrichment of sGSL and vGSL in EhV86 compared with 4-DPI *Ehux374* suggests that they could have been co-localized in the host cell plasma membrane, where Mackinder and colleagues (2009) proposed that EhVs acquire their lipid envelop. Other viruses obtain their lipids from lipid rafts, GSL-enriched plasma-membrane microdomains that are thought to serve as platforms for virus entry and exit (Rajendran and Simons, 2005; Taube *et al.*, 2010; Waheed and Freed, 2010). Rose and colleagues (2014) experimentally isolated lipid raft fractions from *Ehux1516* and found that specific GSL classes were preferentially associated with raft fractions, while other GSL classes were observed in non-raft fractions that included characteristic lipids from intracellular membranes and other plasma membrane components. During infection by EhV86, however, sGSL was initially concentrated in raft fractions, and by 2 DPI, vGSL dominated raft fractions (Rose *et al.*, 2014), supporting our hypothesis that EhV86 acquired sGSL and vGSL together from lipid rafts when budding from the plasma membrane during the early stages of infection.

The sixfold relative enrichment of hGSL in EhV86 compared with 4-DPI *Ehux374* suggests that hGSL was especially concentrated at a site of virus assembly (Fig. 4). As hGSL was always most abundant in non-raft fractions (Rose *et al.*, 2014), EhVs might acquire it during an intracellular assembly step prior to budding from the plasma membrane. We propose that hGSL was acquired during capsid assembly via a mechanism that is similar to that for the hepatitis C virus, which incorporates lipids from the interfaces of lipid bodies and the ER (Herker and Ott, 2011). Lipid bodies in human hepatocyte cells are com-

posed primarily of triacylglycerides (Herker and Ott, 2011); *E. huxleyi* cells contain only small amounts of triacylglycerides but have lipid bodies made up of alkenones instead (Yamamoto *et al*., 2000; Eltgroth *et al*., 2005). We detected C37 and C38 alkenones as the primary neutral lipids in EhV86, and alkenone concentration was twofold greater in the 4-DPI infected population (Fig. 1), possibly indicative of lipid body requirement for virion assembly. Thus, the GSL data are consistent with a two-step lipid addition model, where hGSL would be acquired inside the cell during an initial assembly step prior to vGSL, sGSL and BLL acquisition during budding and exit from the cell.

A two-step model for EhV lipid incorporation would be supported by the occurrence of an internal membrane in addition to the outer envelope. Phycodnaviridae typically have an internal membrane that encapsulates genetic material inside the capsid, and coccolithoviruses are the only genus known to have an outer lipid envelope (Van Etten *et al*., 2002; Mackinder *et al*., 2009). Citing an A32-type ATPase that is encoded by EhV86 and expressed during *E. huxleyi* infection (Wilson *et al*., 2005), Mackinder and colleagues (2009) argued that EhV86 is likely to have an internal membrane in addition to the outer envelope. As nascent EhVs with apparent intact capsids have been observed inside host cells and apart from the plasma membrane (e.g. Bidle *et al*., 2007), it is likely that an internal EhV membrane, possibly comprised largely of hGSL, would be acquired during capsid assembly prior to migration to the plasma membrane.

sGSL and infection susceptibility

sGSL in E. huxleyi *strains.* We examined the GSL content of 27 distinct *E. huxleyi* strains (Supporting Information Table S3), which included five CCMP strains from the National Center for Marine Algae and Microbiota, and 22 'DHB' strains from the Plymouth Culture Collection, the latter of which were isolated during the Raunefjorden mesocosm experiments in June 2008 using single cell sorting (Hinz, 2010; Vardi *et al*., 2012). We found hGSL in all 27 *E. huxleyi* strains, with concentrations ranging between 0.03 and 0.43 fmol cell^{-1} (Supporting Information Table S3), strongly suggesting that all *E. huxleyi* produce hGSL. By contrast, sGSL was not detected in 9 of 27 strains, including two model strains *Ehux373* and *Ehux379*. In the remaining 18 strains, including *Ehux374* and *Ehux1516*, sGSL was present at concentrations up to 0.33 fmol cell^{-1} (Supporting Information Table S3). The two model strains containing sGSL have been consistently identified as being sensitive to EhV infection, while the two model strains that lacked sGSL are resistant to infection (Schroeder *et al*., 2002; Bidle *et al*., 2007; Vardi *et al*., 2009; Bidle and Kwityn, 2012).

We screened seven additional *E. huxleyi* strains for sensitivity to infection by EhV1, EhV86 and EhV163, with sensitivity defined as population crash in the presence of EhVs. DHB 611 and DHB 623 were sensitive to infection by all three EhVs, and CCMP 2090 was sensitive to EhV1 and EhV86 but resistant to EhV163 (Supporting Information Table S3). The other four tested strains (DHB 606, DHB 615, DHB 629 and DHB 641) were resistant to infection by the three EhVs. The three sensitive *E. huxleyi* strains were enriched in sGSL, while the four resistant strains were depleted in sGSL, including three that contained trace concentrations that were too low to be quantified (Fig. 5). These results suggested that sGSL can be used as a biomarker for *E. huxleyi* populations that are sensitive to viral infection, and because hGSL concentration is directly related to total *E. huxleyi* abundance (Vardi *et al*., 2012), we propose that the sGSL/hGSL ratio is a novel and practical diagnostic tool for assessing the infection susceptibility of natural *E. huxleyi* populations. For the 11 strains examined, sGSL/hGSL ratios for sensitive and resistant groups differed significantly (Mann–Whitney $U = 28$, $Z = -2.28$, $P = 0.023$, two-tailed).

The range of sGSL/hGSL ratios in sensitive strains was broad between 0.09 and 2.46 (Fig. 5), so detecting even low sGSL concentrations and sGSL/hGSL ratios in environmental samples would imply that a component of the population is sensitive to infection. Bidle and Kwityn (2012) described a gradient of sensitivity to infection by EhV1, with *Ehux374* > *Ehux1516* > *Ehux373* based on basal caspase specific activity and an infectivity index derived from optical density measurements on infected and uninfected cultures. We found that sGSL content followed the same gradient, with maximum values for *Ehux374* (0.07 fmol cell^{-1}; sGSL/hGSL = 1.10), lower sGSL content for *Ehux1516* (0.02 fmol cell^{-1}; sGSL/hGSL = 0.03) and no sGSL detected in *Ehux373*. Several strains isolated from Raunefjordern had even higher sGSL concentrations than *Ehux374* (Supporting Information Table S3), suggesting that they may have been even more sensitive to infection.

Natural mesocosm populations. In the 2008 Raunefjorden *E. huxleyi* mesocosm bloom experiments, triplicate mesocosm bags 1, 3 and 5 were amended daily with nutrients at the Redfield N : P ratio (15:1) to stimulate growth of natural genotypes, allowing the investigation of a bloom and its subsequent demise via EhV infection (Pagarete *et al*., 2009; Vardi *et al*., 2012). Vardi and colleagues (2012) tracked population changes using hGSL and vGSL as biomarkers, observing direct relationships with *E. huxleyi* and EhV counts respectively. We determined sGSL content for bags 1, 3 and 5 (Fig. 6), finding that the bag 3 population had the greatest initial sGSL content in lag phase, and sGSL increased 25-fold

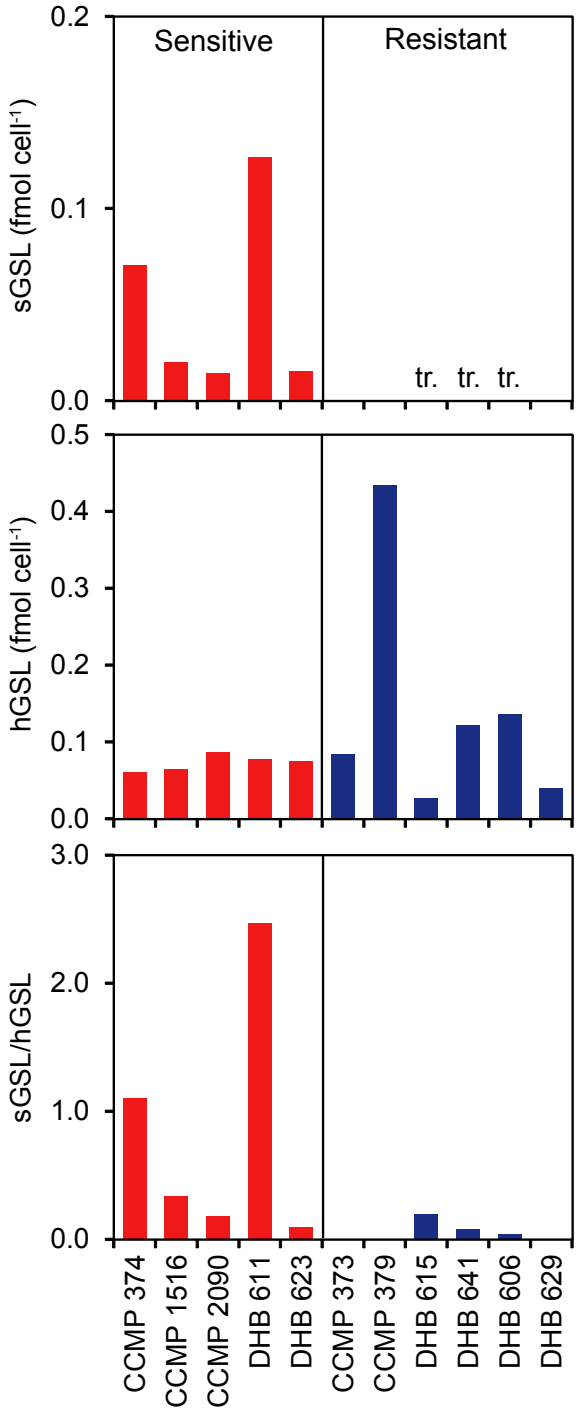

Fig. 5. GSL content of uninfected cultures of 11 strains of *E. huxleyi* that have been tested for EhV infection sensitivity. 'CCMP' strains were obtained from the National Center for Marine Algae and Microbiota, and 'DHB' strains from the Plymouth Culture Collection, having been isolated during the Raunefjorden mesocosm experiments in June 2008.

during exponential growth. At most time points, sGSL content per cell in bag 3 was at least twice that in bags 1 and 5 (Fig. 6).

Based on the observed relationship between sGSL and infectivity in pure cultures (Fig. 5), we would predict that the *E. huxleyi* population in bag 3 was most susceptible to EhV infection. Indeed, bag 3 had the earliest and most intense bloom and demise (Vardi *et al*., 2012), even though the starting population sizes in all three bags were similar (Fig. 6). In addition, virus-induced mortality (VIM), which increased at the end of exponential growth in all three enclosures, was greatest in bag 3, with maximum VIM values of 128% for bag 3, 85% for bag 1 and 62% for bag 5 (Vardi *et al*., 2012). At the end of exponential growth (Phase 2), bag 3 also had the highest sGSL concentration and sGSL/hGSL ratio (Fig. 6 and Supporting Information Fig. S4). Thus, the initial high-sGSL *E. huxleyi* population in bag 3 was sustained into phase 2 of the experiment, leading ultimately to a more intense EhV infection, and an earlier and more intense termination of the *E. huxleyi* bloom.

Observed population declines and calculated VIM in phase 3 point towards infection of most of the *E. huxleyi* population (Vardi *et al*., 2012). Following the gradient of infection sensitivity model (Bidle and Kwityn, 2012), we propose that during exponential growth, the strains with the highest sGSL content were infected at a higher rate than those with less sGSL, leading to preferential lysis of high-sGSL cells and lowering the average sGSL content of the residual *E. huxleyi* population. This would explain the steady decrease in sGSL cell^{-1} observed during exponential growth in bags 1 and 3 as virus counts increased (Fig. 6). Once the host and virus populations reached a critical threshold near the end of phase 2, however, all strains with sGSL would have been readily infected, ultimately terminating the *E. huxleyi* bloom.

sGSL in E. huxleyi *physiology*. Like the other GSLs, sGSL adds an intriguing layer to the co-evolutionary Red Queen dynamic that characterizes *E. huxleyi*-EhV interaction (Van Valen, 1973; Bidle and Vardi, 2011). The proposed occurrence of sGSL on the plasma membrane would suggest that it could have structural and physical roles as well as being a binding site for extrinsic and intrinsic receptors (Varki, 2008). KDN, which is the novel monosaccharide sialic acid headgroup of sGSL, has been detected in a variety of aquatic organisms, notably in fish gamete cells, fish skin mucus and amphibian egg coatings, as well as in pathogenic bacteria, plant rhizobia and plant pathogens (Inoue and Kitajima, 2006). Sialic acids are common on the outer leaflet of eukaryotic cell membranes. Positioned as terminal groups on gangliosides and glycoproteins, sialic acids facilitate polar hydrogen bonds and salt bridges and also participate in non-polar

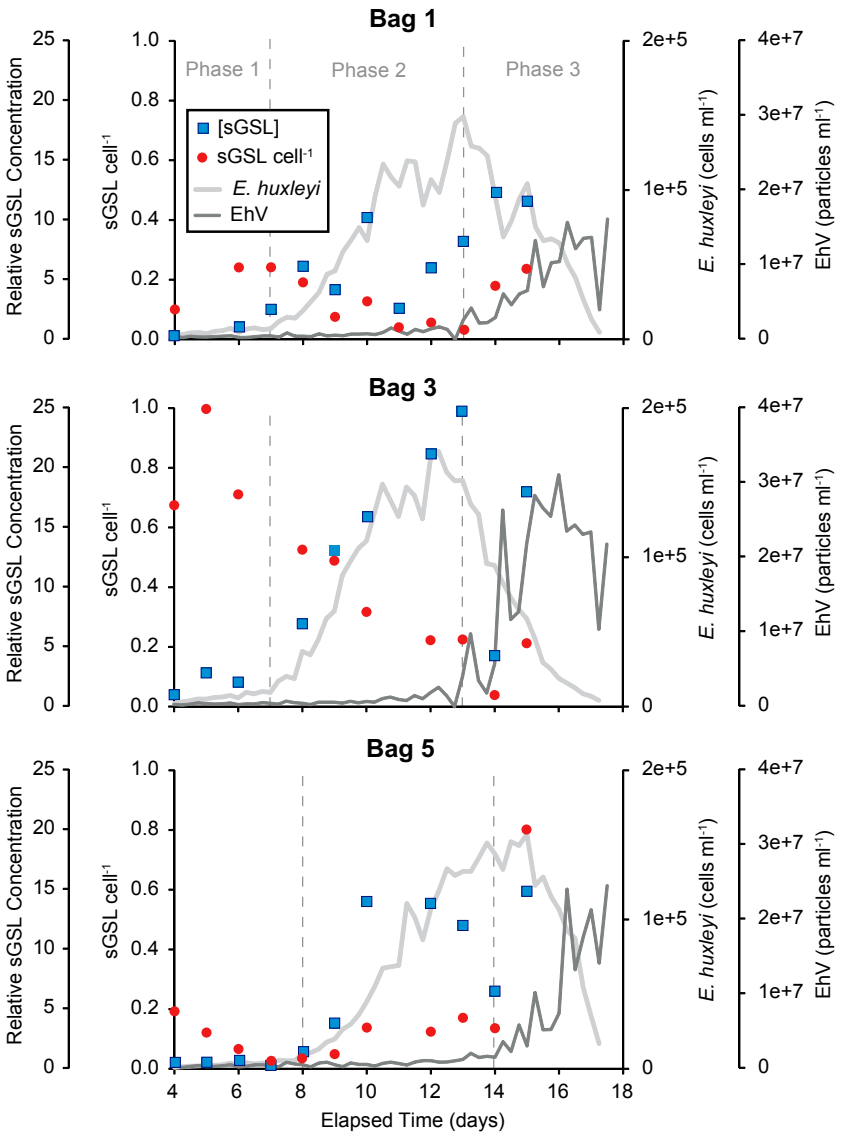

Fig. 6. sGSL in Raunefjorden mesocosm bags 1, 3 and 5 (June 2008). To allow comparison among the three enclosures, we report sGSL content in all bags relative to its concentration in bag 3 on day 4, the first day it was measured. We normalized sGSL cell^{-1} to the maximum value, which was on day 5 in bag 3. Growth phase 1 was lag phase with low *E. huxleyi* abundance, phase 2 was exponential growth, and phase 3 included *E. huxleyi* demise and EhV proliferation.

interactions (Neu *et al.*, 2011), binding with extracellular molecules and ions (Varki, 1997; Varki and Schauer, 2009).

If KDN in sGSL is indeed a target of hydrolysis by EhV sialidases and/or a ligand for attachment by EhV lectin proteins, then the *E. huxleyi*-EhV interaction could share similarities with infection by a range of human pathogens, including many species of enveloped (e.g. influenza A, B and C, and parainfluenza viruses) and non-enveloped viruses (e.g. type D adenoviruses, and JC and BK polyomaviruses) that exploit host cell sialic acid moieties (Stray *et al.*, 2000; Neu *et al.*, 2011). Neu5Ac, which is simply the aminated form of KDN, has been studied broadly in this context, being a known ligand for viral receptors in the human system (Varki, 1997). More recently, Neu5Ac was identified as a ligand for viral infection of the marine cyanobacterium *Prochlorococcus* (Avrani *et al.*, 2011). Less is known about KDN as a vial receptor, although plant lectins have been identified that show preference for KDN over Neu5Ac (Song *et al.*, 2011). The EhV86 genome encodes two C-type lectin domain-containing proteins with unknown affinities that were also detected in mature virions (Wilson *et al.*, 2005; Allen *et al.*, 2008), and one of these proteins, ehv149, was also enriched in a lipid raft fraction isolated from 2 h EhV86-infected *Ehux1516* cells (Rose *et al.*, 2014), increasing the likelihood of their involvement in EhV infection.

Intrinsic functions for sGSL may include involvement in calcite coccolith emplacement on the cell exterior, where coccoliths are attached by acidic polysaccharides that could interact with sGSL (Kayano and Shiraiwa, 2009). Sialic acids have particular affinity for Ca^{2+} ions (Shimoda *et al.*, 1994; Ziak *et al.*, 1999), and the sGSL headgroup could also serve as a ligand for concentrating extracellular

Ca^{2+}. Alternatively, an intracellular occurrence of sGSL in the coccolith vesicle could be a scaffold for coccolith assembly, with sGSL accompanying coccoliths to the cell periphery and plasma membrane (Westbroek *et al*., 1984). Wilson and colleagues (2009) even suggested that EhVs might exit host cells by taking advantage of the export machinery that transfers coccoliths to the cell periphery, further connecting sGSL with both coccoliths and coccolithoviruses. While the suggested role for sGSL in coccolith production and emplacement is speculative, regardless of its endogenous function, sGSL content per cell was greatest in the mesocosm bag with the earliest and most intense *E. huxleyi* bloom (Fig. 6), suggestive of a possible link between sGSL content and cell fitness. While specific growth rates of strains with and without sGSL (*Ehux373*, *Ehux374*, *Ehux379* and *Ehux1516*) were indistinguishable (Bidle and Kwityn, 2012), direct competition among different strains could reveal a cost of resistance for lacking sGSL, providing an evolutionary advantage to *E. huxleyi* cells with sGSL and explaining the persistence of sGSL biosynthesis in light of its involvement in EhV infection.

Experimental procedures

Ehux374 cultures

Batch cultures of *E. huxleyi* strain CCMP 374 were grown in 1 l polycarbonate bottles with L1-Si medium at 18°C and a 12:12 h light : dark illumination cycle at ~60 μE s^{-1} m^{-2} irradiance. One-ml aliquots were taken daily for cell abundance determination by Multisizer 3 Coulter Counter (Beckman Coulter, Inc., Indianapolis, IN, USA). When the cultures reached an average density of approximately 4×10^5 cells ml^{-1} (Day 0), they were inoculated with EhV86 lysate to a multiplicity of infection (MOI) of 5. Infected and control cultures were maintained for 4 DPI, when the infected host population had crashed and the control cultures were in late exponential phase. Fifteen-millilitre aliquots were taken daily from each culture tube and filtered onto precombusted 25-mm diameter GF/F glass fiber filters, which were snap-frozen in liquid nitrogen and transferred to a freezer for storage at −80°C prior to lipid analysis.

Virus isolation

Virus particles were isolated from a 20 l CCMP 374 culture (f/2-Si medium; 14:10 h light : dark) that was infected by EhV86 at a MOI of 5. Vardi and colleagues (2009) provided details of the isolation protocol, which is described here briefly. Five days post-infection, the infected culture lysate was filtered through a 0.45-μm pore-size Sterivex filter using a peristaltic pump, and EhVs in the filtrate were concentrated to 50 ml by tangential flow filtration (VivaFlow200; 50 kD, Sartorius, Bohemia, NY, USA). Final purification employed $CsCl_2$ gradient ultracentrifugation (176 000 × *g*) with the virus band extracted by syringe, filtered onto precombusted, 0.02 μm pore-size Anodisc filters and snap-frozen in liquid nitrogen. EhV purification was verified both by SYBR Green staining, and flow cytometry and epifluorescence microscopy, as well as via PCR with EhV-specific major capsid protein primers (Vardi *et al*., 2009).

Mesocosms

The Raunefjorden (Norway) mesocosm experiments were conducted from June 5 to June 21, 2008 at the University of Bergen Marine Biological Station (60.38°N, 5.28°E). Similar mesocosm experiments have been carried out at this location for two decades (Egge and Herndl, 1994), and the details of the 2008 experimental design have been described (Pagarete *et al*., 2009; Vardi *et al*., 2012). Briefly, unfiltered water was pumped from 10 m depth into polyethylene mesocosm bags (11 m^3) that were moored at the surface, isolating the water to a depth of 4 m. $NaNO_3$ and KH_2PO_4 were added daily to bags 1, 3 and 5 with concentrations of 1.5 μM NO_3^- and 0.1 μM PO_4^{3-} (N : *P* = 15 : 1). *Emiliania huxleyi* cells and coccolithoviruses were counted every 6 h by flow cytometry (Pagarete *et al*., 2009; Vardi *et al*., 2012), and water samples (5 l) were taken daily for lipid analysis (Vardi *et al*., 2012), with particles collected on precombusted GF/F filters, snap-frozen in liquid nitrogen and stored at −80°C in preparation for analysis.

Lipid analysis

Total lipid extracts (TLEs) were extracted using a modified Bligh and Dyer method, with the internal recovery standard 1,2-dipalmitoyl-*sn*-glycero-3-phosphoethanolamine-N-(2,4-dinitrophenyl) (DNP-PE) added to facilitate quantitation (Bligh and Dyer, 1959; Popendorf *et al*., 2013). IPLs were analysed by HPLC-MS^n on a Hewlett Packard 1100 HPLC (Agilent Technologies, Santa Clara, CA, USA) and LCQ Deca XP ion-trap mass spectrometer (ThermoFinnigan, San Jose, CA, USA) with electrospray ionization (Sturt *et al*., 2004). Polar glycerolipid and GSL peaks were identified by retention time, and MS^2 and MS^3 fragmentation patterns compared with previous analyses using the same methods (Vardi *et al*., 2009; Van Mooy and Fredricks, 2010). The molecular ions, and MS^2 and MS^3 fragment ions for the novel lipids sGSL, PDPT and BLL were identified first by ion trap MS. Then, using the same chromatographic method, molecular and MS^2 ions were analysed on a Thermo LTQ FT Ultra high-resolution Fourier-transform ion cyclotron resonance mass spectrometer, allowing the accurate mass determination of molecular ions and headgroups.

IPLs were quantified based on molecular ion peak areas (Van Mooy and Fredricks, 2010), using linear response factors for PC, PE, PG and DNP-PE (Avanti Polar Lipids, Alabaster, AL, USA); MGDG and DGDG (Matreya LLC, Pleasant Gap, PA, USA); and SQDG (Lipid Products, South Nutfield, UK). New response factors were calculated for each set of analyses, and quality control standards were analysed between groups of five samples to account for instrument drift and variable ionization efficiency. For sGSL, hGSL and vGSL, quantitation was based on a response factor for glucocerebrosides (soy, Avanti Polar Lipids), which has a similar chemical structure and sugar headgroup that accepts a positive charge in the ion source. The response factor for

PC was applied to PDPT, BLL, DGCC and DGTS, as these compounds are not available commercially and have similar structures and zwitterionic properties as PC. Past analysis of DGCC and DGTS purified from algal cultures has shown that their response factors vary by less than 50% from PC, so concentrations calculated for these compounds are probably better than ± 50%, and we would estimate similar maximum uncertainty for PDPT and BLL. All other polar glycerolipid concentrations are estimated to be accurate within 10–15% (Van Mooy and Fredricks, 2010).

For gas chromatographic (GC) analysis of alkenones, 1 ml aliquots (50%) of the TLE were transferred to 40 ml vials, dried under N_2 and dissolved in 0.5 ml hexane. Ethyl tricosanoate and n-heptadecane were added as internal and external standards, respectively, and 2 ml anhydrous methanolic HCl was added to transesterify/methylate carboxylic acid moieties and derivatize compounds that can coellute with alkenones (Conte *et al*., 1992). The sealed vials were heated at 65°C for 14–16 h under N_2, after which 10 ml of deionized water (MilliQ, Millipore, Billerica, MA, USA) and 10 ml of hexane were added for phase separation. The non-polar phases were transferred to clean vials, and after concentrating to 0.1–1.0 ml under a stream of N_2, the solutions were analysed by GC-flame ionization detection on a Hewlett Packard 5890 Series II GC equipped with a 7673 GC/SFC injector. Alkenones were quantified using a linear response factor for a standard alkenone mixture derived from *Isochrysis galbana*.

Acknowledgments

The authors acknowledge Melissa Kido Soule of the Woods Hole Oceanographic Institution FT-MS Facility and Catherine Carmichael for analytical assistance. Rutgers undergraduate students Ashley Lemire and Chris Johns helped screen the infectivity of Bergen mesocosm *E. huxleyi* strains and Jennifer Rusciani assisted in EhV86 purification. We also thank Dr. Chris Brown and Liti Haramaty for technical assistance. Funding support for this study came from National Science Foundation grants (OCE- 1031143 to B.A.S.V.M.; OCE-1061883 to K.D.B., B.A.S.V.M., G.R.D. and A.V.; IOS-0717494 to K.D.B and A.V). This research was funded in part by the Gordon and Betty Moore Foundation. The authors have no conflicts of interest pertinent to this research.

References

Allen, M.J., Howard, J.A., Lilley, K.S., and Wilson, W.H. (2008) Proteomic analysis of the EhV-86 virion. *Proteome Sci* **6:** 11.

Avrani, S., Wurtzel, O., Sharon, I., Sorek, R., and Lindell, D. (2011) Genomic island variability facilitates *Prochlorococcus*-virus coexistence. *Nature* **474:** 604–608.

Bell, M.V., and Pond, D. (1996) Lipid composition during growth of motile and coccolith forms of *Emiliania huxleyi*. *Phytochemistry* **41:** 465–471.

Bidle, K.D., and Kwityn, C.J. (2012) Assessing the role of caspase activity and metacapsase expression on viral susceptibility of the coccolithophore, *Emiliania huxleyi* (Haptophyta). *J Phycol* **48:** 1079–1089.

Bidle, K.D., and Vardi, A. (2011) A chemical arms race at sea mediates algal host-virus interactions. *Curr Op Microbio* **14:** 449–457.

Bidle, K.D., Harmaty, L., Barcelos e Ramos, J., and Falkowski, P. (2007) Viral activation and recruitment of metacaspases in the unicellular coccolithophore, *Emiliania huxleyi*. *Proc Natl Acad Sci U S A* **104:** 6049–6054.

Bligh, E.G., and Dyer, W.J. (1959) A rapid method of total lipid extraction and purification. *Can J Biochem Physiol* **37:** 911–917.

Bratbak, G., Egge, J.K., and Heldal, M. (1993) Viral mortality of the marine alga *Emiliania huxleyi* (Haptophyceae) and termination of algal blooms. *Mar Ecol Prog Ser* **93:** 39–48.

Brugger, B., Glass, B., Haberkant, P., Leibrecht, I., Wieland, F.T., and Krasslich, H.G. (2006) The HIV lipidome: a raft with an unusual composition. *Proc Natl Acad Sci U S A* **103:** 2641–2646.

Brussaard, C.P.D., Wilhelmd, S.W., Thingstadd, F., Weinbauerd, M.G., Bratbakd, G., Heldald, M., *et al*. (2008) Global-scale processes with a nanoscale drive: the role of marine viruses. *ISME J* **2:** 575–578.

Conte, M.H., Eglinton, G., and Madureira, L.A.S. (1992) Long-chain alkenones and alkyl alkenoates as palaeotemperature indicators: their production, flux and early sedimentary diagenesis in the Eastern North Atlantic. *Org Geochem* **19:** 287–298.

Dembitsky, V.M. (1996) Betaine ether-linked glycerolipids: chemistry and biology. *Prog Lipid Res* **35:** 1–51.

Egge, J.K., and Herndl, G.J. (1994) Blooms of *Emiliania huxleyi* (Haptophyta) in mesocosm experiments: effects of nutrient supply in different N : P ratios. *Sarsia* **79:** 333–348.

Eltgroth, M.L., Watwood, R.L., and Wolfe, G.V. (2005) Production and cellular localization of neutral long-chain lipids in the haptophyte algae *Isochrysis galbana* and *Emiliania huxleyi*. *J Phycol* **41:** 1000–1009.

Evans, C., Malin, G., and Mills, G.P. (2006) Viral infection of *Emiliania huxleyi* (Prymnesiophyceae) leads to elevated production of reactive oxygen species. *J Phycol* **42:** 1040–1047.

Evans, C., Pond, D.W., and Wilson, W.H. (2009) Changes in *Emiliania huxleyi* fatty acid profiles during infection with *E. huxleyi* virus 86: physiological and ecological implications. *Aquat Microb Ecol* **55:** 219–228.

Fuhrman, J.A. (1999) Marine viruses and their biogeochemical and ecological effects. *Nature* **399:** 541–548.

Guschina, I.A., and Harwood, J.L. (2006) Lipids and lipid metabolism in eukaryotic algae. *Prog Lipid Res* **45:** 160–186.

Han, G.S., Gable, K., Yan, L.Y., Allen, M.J., Wilson, W.H., Moitra, P., *et al*. (2006) Expression of a novel marine viral single-chain serine palmitoyltransferase and construction of yeast and mammalian single-chain chimera. *J Biol Chem* **281:** 39935–39942.

Harwood, J.L., and Jones, A.L. (1989) Lipid-metabolism in algae. *Adv Bot Res* **16:** 1–53.

Herker, E., and Ott, M. (2011) Unique ties between hepatitis C virus replication and intracellular lipids. *Trends Endocrin Metab* **22:** 241–248.

Hinz, D.J. (2010) *Emiliania huxleyi* and climate change: a genetic and biogeographic investigation of bloom dynamics for a key phytoplankton species in the global carbon cycle. PhD Thesis. Southampton, UK: University of Southampton, School of Ocean & Earth Science.

Inoue, S., and Kitajima, K. (2006) KDN (deaminated neuraminic acid): dreamful past and exciting future of the newest member of the sialic acid family. *Glycoconj J* **23:** 277–290.

Kato, M., Sakai, M., Adachi, K., Ikemoto, H., and Sano, H. (1996) Distribution of betaine lipids in marine algae. *Phytochemistry* **42:** 1341–1345.

Kayano, K., and Shiraiwa, Y. (2009) Physiological regulation of coccolith polysaccharide production by phosphate availability in the coccolithophorid *Emiliania huxleyi*. *Plant Cell Physiol* **50:** 1522–1531.

Mackinder, L.C.M., Worthy, C.A., Biggi, G., Hall, M., Ryan, K.P., Varsani, A., *et al*. (2009) A unicellular algal virus, *Emiliania huxleyi* virus 86, exploits an animal-like infection strategy. *J Gen Virol* **90:** 2306–2316.

Merz, A., Long, G., Hiet, M.S., Brugger, B., Chlanda, P., Andre, P., *et al*. (2011) Biochemical and morphological properties of hepatitis C virus particles and determination of their lipidome. *J Biol Chem* **286:** 3018–3032.

Neu, U., Bauer, J., and Stehle, T. (2011) Viruses and sialic acids: rules of engagement. *Curr Op Struct Biol* **21:** 610–618.

Pagarete, A., Allen, M.J., Wilson, W.H., Kimmance, S.A., and de Vargas, C. (2009) Host-virus shift of the sphingolipid pathway along an *Emiliania huxleyi* bloom: survival of the fattest. *Environ Microbiol* **11:** 2840–2848.

Passow, U., Shipe, R.F., Murray, A., Pak, D.K., Brzezinski, M.A., and Alldredge, A.L. (2001) The origin of transparent exopolymer particles (TEP) and their role in the sedimentation of particulate matter. *Cont Shelf Res* **21:** 327–346.

Popendorf, K.J., Lomas, M.W., and Van Mooy, B.A.S. (2011) Microbial sources of intact polar diacylglycerolipids in the Western North Atlantic Ocean. *Org Geochem* **42:** 803–811.

Popendorf, K.J., Fredricks, H.F., and Van Mooy, B.A.S. (2013) Molecular ion-independent quantification of polar glycerolipid classes in marine plankton using triple quadrupole MS. *Lipids* **48:** 185–195.

Rajendran, L., and Simons, K. (2005) Lipid rafts and membrane dynamics. *J Cell Sci* **118:** 1099–1102.

Rose, S.L., Fulton, J.M., Brown, C.M., Natale, F., Van Mooy, B.A.S., and Bidle, K.D. (2014) Isolation and characterization of lipid rafts in *Emiliania huxleyi*: a role for membrane microdomains in host-virus interactions. Submitted to *Env Microbiol* doi:10.1111/1462-2920.12357.

Scheiffele, P., Rietveld, A., Wilk, T., and Simons, K. (1999) Influenza viruses select ordered lipid domains during budding from plasma membrane. *J Biol Chem* **274:** 2038–2044.

Schroeder, D.C., Oke, J., Malin, G., and Wilson, W.H. (2002) Coccolithovirus (*Phycodnaviridae*): characterisation of a new large dsDNA algal virus that infects *Emiliana huxleyi*. *Arch Virol* **147:** 1685–1698.

Shimoda, Y., Kitajima, K., Inoue, S., and Inoue, Y. (1994) Calcium ion binding of three different types of oligo/polysialic acids as studied by equilibrium dialysis and circular dichroic methods. *Biochemistry* **33:** 1202–1208.

Song, X., Yu, H., Chen, X., Lasanajak, Y., Tappert, M.M., Air, G.M., *et al*. (2011) A sialylated glycan microarray reveals novel interactions of modified sialic acids with proteins and viruses. *J Biol Chem* **286:** 31610–31622.

Stray, S.J., Cummings, R.D., and Air, G.M. (2000) Influenza virus infection of desialylated cells. *Glycobiology* **10:** 649–658.

Sturt, H.F., Summons, R.E., Smith, K., Elvert, M., and Hinrichs, K.U. (2004) Intact polar membrane lipids in prokaryotes and sediments deciphered by high-performance liquid chromatography/electrospray ionization multistage mass spectrometry – new biomarkers for biogeochemistry and microbial ecology. *Rapid Commun Mass Spectrom* **18:** 617–628.

Suttle, C.A. (2007) Marine viruses – major players in the global ecosystem. *Nat Rev Microbiol* **5:** 801–812.

Taube, S., Jiang, M., and Wobus, C.E. (2010) Glycosphingolipids as receptors for non-enveloped viruses. *Viruses* **2:** 1011–1049.

Thyrhaug, R., Larsen, A., Thingstad, T.F., and Bratbak, G. (2003) Stable coexistence in marine algal host-virus systems. *Mar Ecol Prog Ser* **254:** 27–35.

Van Etten, J.L., Graves, M.V., Muller, D.G., Boland, W., and Delaroque, N. (2002) Phycodnaviridae – large DNA algal viruses. *Arch Virol* **147:** 1479–1516.

Van Mooy, B.A.S., and Fredricks, H.F. (2010) Bacterial and eukaryotic intact polar lipids in the eastern subtropical South Pacific: water-column distribution, planktonic sources, and fatty acid composition. *Geochim Cosmochim Acta* **74:** 6499–6516.

Van Mooy, B.A.S., Fredricks, H.F., Pedler, B.E., Dyhrman, S.T., Karl, D.M., Koblizek, M., *et al*. (2009) Phytoplankton in the ocean use non-phosphorus lipids in response to phosphorus scarcity. *Nature* **458:** 69–72.

Van Valen, L. (1973) A new evolutionary law. *Evol Theory* **11:** 1–30.

Vardi, A., Van Mooy, B.A.S., Fredricks, H.F., Popendorf, K.J., Ossolinski, J.E., Haramaty, L., and Bidle, K.D. (2009) Viral glycosphingolipids induce lytic infection and cell death in marine phytoplankton. *Science* **326:** 861–865.

Vardi, A., Haramaty, L., Van Mooy, B.A.S., Fredricks, H.F., Kimmance, S., Larsen, A., and Bidle, K.D. (2012) Host-virus dynamics and subcellular controls of cell fate in a natural coccolithophore population. *Proc Natl Acad Sci U S A* **109:** 19327–19332.

Varki, A. (1997) Sialic acids as ligands in recognition phenomena. *FASEB J* **11:** 248–255.

Varki, A. (2008) Sialic acids in human health and disease. *Trends Molec Med* **14:** 351–360.

Varki, A., and Schauer, R. (2009) Sialic acids. In *Essentials of Glycobiology*. Varki, A., Cummings, R.D., Esko, J.D., Freeze, H.H., Stanley, P., Bertozzi, C.R., *et al*. (eds). Cold Springs Harbor, NJ, USA: Cold Springs Harbor Laboratory Press, pp. 199–218.

Waheed, A.A., and Freed, E.O. (2010) The role of lipids in retrovirus replication. *Viruses* **2:** 1146–1180.

Westbroek, P., Dejong, E.W., Vanderwal, P., Borman, A.H., Devrind, J.P.M., Kok, D., *et al*. (1984) Mechanism of calcification in the marine alga *Emiliania huxleyi*. *Philos Trans R Soc Lond Ser B-Biol Sci* **304:** 435–444.

Wilhelm, S.W., and Suttle, C.A. (1999) Viruses and nutrient cycles in the sea – viruses play critical roles in the structure and function of aquatic food webs. *Bioscience* **49:** 781–788.

Wilson, W.H., Tarran, G., and Zubkov, M.V. (2002a) Virus dynamics in a coccolithophore-dominated bloom in the North Sea. *Deep Sea Res Part 2 Top Stud Oceanogr* **49:** 2951–2963.

Wilson, W.H., Tarran, G.A., Schroeder, D., Cox, M., Oke, J., and Malin, G. (2002b) Isolation of viruses responsible for the demise of an *Emiliania huxleyi* bloom in the English Channel. *J Mar Biol Ass UK* **82:** 369–377.

Wilson, W.H., Schroeder, D.C., Allen, M.J., Holden, M.T.G., Parkhill, J., Barrell, B.G., *et al*. (2005) Complete genome sequence and lytic phase transcription profile of a coccolithovirus. *Science* **309:** 1090–1092.

Wilson, W.H., Van Etten, J.L., and Allen, M.J. (2009) The *Phycodnaviridae*: the story of how tiny giants rule the world. *Curr Top Microbiol Immunol* **328:** 1–42.

Yamamoto, M., Shiraiwa, Y., and Inouye, I. (2000) Physiological responses of lipids in *Emiliania huxleyi* and *Gephyrocapsa oceanica* (Haptophyceae) to growth status and their implications for alkenone paleothermometry. *Org Geochem* **31:** 799–811.

Ziak, M., Kerjaschki, D., Farquhar, M.G., and Roth, J. (1999) Identification of megalin as the sole rat kidney sialoglycoprotein containing poly α2,8 deaminoneuraminic acid. *J Amer Soc Nephrol* **10:** 203–209.

Supporting information

Additional Supporting Information may be found in the online version of this article at the publisher's web-site:

Appendix S1. Intact polar lipid structural assignment.

Fig. S1. Ion trap MS^2 positive ion mass spectrum of the m/z 870 sGSL molecular ion. The MS^2 mass spectrum of sGSL is similar to other glycosphingolipids, with headgroup and water neutral losses accounting for the m/z 620, 602 and 584 ions. The major neutral losses of 268 and 250 Da reveal that the headgroup is larger than a simple sugar. The m/z 340 and 262 MS^2 ions indicate that sGSL has a C22:0 fatty acid and d18:2 long-chain base. Accurate mass determination by FT-ICR-MS showed that the molecular ion has m/z 870.66535, supporting a molecular formula of $C_{49}H_{92}O_{11}N^+$ ($\delta = -1.308$ ppm), and that the main MS^2 ions have m/z 620.59733 ($C_{40}H_{78}O_3N^+$; $\delta = -0.470$ ppm), m/z 602.58694 Da ($C_{40}H_{76}O_2N^+$; $\delta = -0.194$ ppm), m/z 584.57937 ($C_{40}H_{74}ON^+$; $\delta = 4.922$ ppm) and m/z 262.25294 ($C_{18}H_{32}N^+$; $\delta = 0.051$ ppm). We did not detect the 340 Da amino fatty acid by high-resolution MS. The headgroup neutral loss (870.66535–602.58694 = 268.07841 Da) supports the formula $C_9H_{16}O_9$ ($\delta = -1.766$ ppm), which is the same as the sialic acid 2-Keto-3-deoxynonic acid (Kdn).

Fig. S2. FT-ICR-MS MS^3 negative ion mode mass spectrum of the sGSL headgroup. In negative ion mode, sGSL was detected with m/z 868.65134 ($C_{49}H_{90}O_{11}N^-$, $\delta = 0.557$ ppm). The MS^2 product ion with m/z 249.06140 supports a formula of $C_9H_{13}O_8^-$ ($\delta = 0.861$ ppm), which suggests the retention of the ether-linking oxygen on ceramide and the transfer of hydrogen from the negative ion and the subsequent C = C double-bond formation. The most abundant MS^3 fragment ions have m/z 129.01923 ($C_5H_5O_4^-$, $\delta = 7.711$ ppm) and m/z 87.00870 ($C_3H_3O_3^-$, $\delta = 11.832$). Their requirement of three and two double bonds, respectively, suggests that they most likely include the carboxyl moiety and derive from ring cleavage.

Fig. S3. FT-ICR-MS MS^2 and MS^3 negative ion mode mass spectra for 2-Keto-3-deoxynonic acid (KDN). Panel A is the MS^2 spectrum of the m/z 267.07221 MS parent ion, showing two water losses (m/z 249.06149 and 231.05091) and m/z 129.01923 and 87.00864 ions similar to those in the sGSL MS^3 spectrum (Supporting Information Fig. S2). The m/z 249.06149 ion likely results from dehydration at the C_2 position with a double bond formed between C_2 and C_3. Panel B is the MS^3 spectrum of the m/z 249.06149 MS^2 ion, which is dominated by a m/z 129.01922 product, similar to the sGSL MS^3 spectrum in Fig. S2, supporting our assignment of the single sialic acid KDN headgroup for sGSL.

Fig. S4. Ratios of sGSL/hGSL in mesocosm bags 1, 3 and 5. Growth phase 1 is lag phase, phase 2 is exponential growth, and phase 3 includes *E. huxleyi* demise and EhV proliferation.

Table S1. Increasing lipids in infected *Ehux374*.

Table S2. Fatty acid components of IPLs from CCMP 374, EhV86-infected CCMP 374 and EhV86.

Table S3. Glycosphingolipid content of *E. huxleyi* strains in culture.